On the kinetics of MoSe2 interfacial layer formation in chalcogen-based thin film solar cells with a molybdenum back contact

Byungha Shin, Nestor A. Bojarczuk, and Supratik Guha

Articles you may be interested in

Enhancing the Cu2ZnSnS4 solar cell efficiency by back contact modification: Inserting a thin TiB2 intermediate layer at Cu2ZnSnS4/Mo interface
Appl. Phys. Lett. **104**, 051105 (2014); 10.1063/1.4863736

Alternative back contacts in kesterite Cu2ZnSn(S1-xSex)4 thin film solar cells
J. Renewable Sustainable Energy **6**, 011401 (2014); 10.1063/1.4831781

Control of an interfacial MoSe2 layer in Cu2ZnSnSe4 thin film solar cells: 8.9% power conversion efficiency with a TiN diffusion barrier
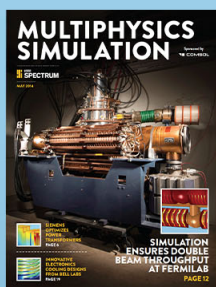Appl. Phys. Lett. **101**, 053903 (2012); 10.1063/1.4740276

Study of molybdenum back contact layer to achieve adherent and efficient CIGS2 absorber thin-film solar cells
J. Vac. Sci. Technol. A **23**, 1197 (2005); 10.1116/1.1889440

Enhanced back reflectance and quantum efficiency in Cu (In , Ga) Se 2 thin film solar cells with a ZrN back reflector
Appl. Phys. Lett. **85**, 2634 (2004); 10.1063/1.1794860

On the kinetics of MoSe₂ interfacial layer formation in chalcogen-based thin film solar cells with a molybdenum back contact

Byungha Shin, Nestor A. Bojarczuk, and Supratik Guha
IBM T. J. Watson Research Center, Yorktown Heights, New York 10598, USA

We have studied the temperature dependent kinetics of MoSe$_2$ formation between molybdenum and Cu$_2$ZnSnSe$_4$ (CZTSe) films during annealing in the presence of Se. CZTSe is an emerging light-absorbing material for thin film solar cell applications, and thermal treatment of this layer constitutes a critical part of the device processing. The formation of MoSe$_2$ in this system is modeled using a three step mechanism—diffusion of Se through CZTSe, diffusion of Se through MoSe$_2$, and reaction between Se and Mo. Applying the results of the model to experimental results reveals that the MoSe$_2$ formation is limited by the diffusion of Se through the CZTSe layer. © *2013 American Institute of Physics.* [http://dx.doi.org/10.1063/1.4794422]

Thin film solar cells using the absorber materials Cu$_2$ZnSn(S$_x$Se$_{1-x}$)$_4$ (CZTSSe) have received a lot of recent attention due to the earth abundant nature of the constituents of this compound.[1–3] Solar cells fabricated with CZTSSe have a device stack comparable to other thin film chalcogen-based solar cells such as CdTe and Cu(In,Ga)Se$_2$ (CIGS)—the absorber is deposited on a bottom molybdenum electrode, and usually a CdS emitter layer is used at the front surface. As with the case for CIGS based devices, an anneal or high temperature step (>500 °C) during CZTSSe device fabrication is usually necessary and carried out in the presence of a chalcogen overpressure (to prevent the possible loss of volatile chalcogen species from the absorber). During this process, the molybdenum back electrode reacts with the chalcogen to form an interfacial MoSe$_2$ (or MoS$_2$) layer.[4] It has important consequences on device performance—it has been claimed to assist the formation of Ohmic contact when its thickness is less than a few hundred nanometers,[4] while excessive thicknesses have been shown to adversely affect solar cell performances.[1,5] Understanding of the formation kinetics of MoSe$_2$ is, therefore, not only of scientific interest but also bears practical interest (such as improving the solar cell performance by controlling the interfacial MoSe$_2$ layer thickness). In this work, we have studied the formation of a MoSe$_2$ interfacial layer between a pure selenide CZTSe (i.e., Cu$_2$ZnSnSe$_4$) absorber and a Mo back contact.

A CZTSe absorber was prepared on a Mo-coated glass substrate by thermal co-evaporation, at a substrate temperature of 150 °C, using Knudsen-type sources for elemental Cu, Zn, and Sn, and a commercially available valved-cracker for Se. Further details of the growth conditions can be found elsewhere.[2] Following the deposition, samples received annealing under a Se ambient. The Se partial pressure during the post-deposition annealing was maintained higher than an equilibrium vapor pressure of Se at a given annealing temperature by keeping pieces of elemental Se at a temperature higher than the annealing temperature. The annealing temperature was varied from 480 to 540 °C and the duration from 90 to 400 s.

Figure 1(a) presents a scanning electron microscopy (SEM) image of a CZTSe/Mo structure that was annealed at 480 °C for 180 s. The formation of an interfacial layer of ~550 nm is evident between CZTSe and Mo.[6] An X-ray diffraction (XRD) measurement in theta–2 theta mode [Fig. 1(b)] taken from a similarly prepared sample (annealed at 540 °C for 180 s) reveals two peaks other than those belong to the Mo or the CZTSe (marked by asteroids in the figure), which match to MoSe$_2$ reflections.[7] The absence of MoSe$_2$ (00n) reflections suggests that the c-axis of the MoSe$_2$ layer is parallel to the Mo surface, which is known to promote good adhesion between CZTSe and Mo.[4]
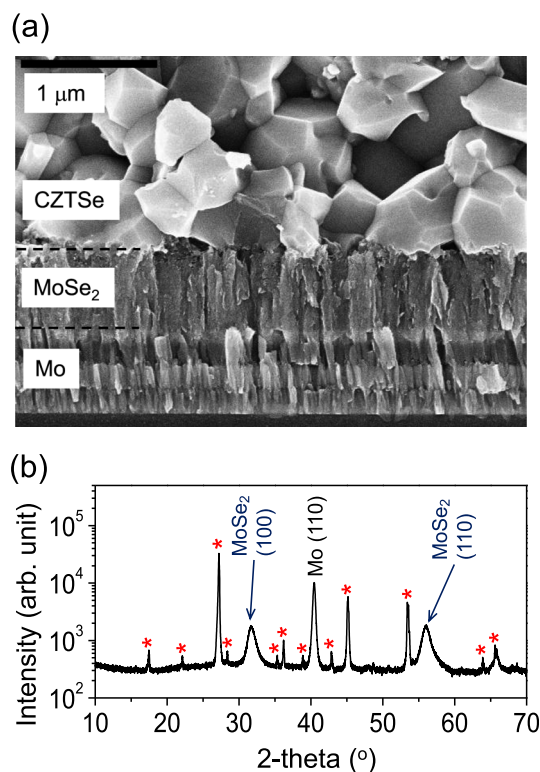

(a)

(b)

FIG. 1. (a) SEM image of CZTSe absorber grown on Mo-coated glass that was annealed at 480 °C for 180 s, which illustrates the formation of an interfacial MoSe$_2$ layer between CZTSe and Mo. (b) XRD pattern from a CZTSe/Mo annealed at 540 °C. Peaks marked by "*" are from CZTSe. Two broad peaks at ~31.6° and 56° belong to MoSe$_2$.
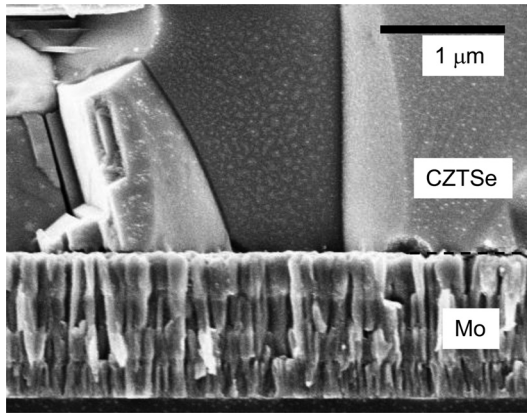
102, 091907-1

FIG. 2. SEM image of CZTSe/Mo that was annealed at 570 °C for 180 s without any external supply of Se vapor during annealing. No MoSe$_2$ inter-facial layer is observed within the resolution of SEM.

No MoSe$_2$ layer is observed when the sample is annealed under inert conditions with no supply of Se vapor. This can be seen in the SEM micrograph of Fig. 2 for a sample annealed in the absence of a Se ambient (note that the grain size of Fig. 2 is larger than that of Fig. 1(a) because of different annealing temperatures used—570 °C for Fig. 2 vs. 480 °C for Fig. 1(a)). One may therefore conclude that the Mo layer does not reduce the CZTSe layer to any appreciable extent. Therefore, the formation of the MoSe$_2$ involves the following steps: (i) condensation of Se vapor onto the CZTSe surface, followed by diffusion of Se through the CZTSe layer; (ii) diffusion of Se through the growing MoSe$_2$ layer,[8] and (iii) the reaction of Se atoms that have arrived at the MoSe$_2$/Mo interface with Mo to form MoSe$_2$. In the following, we develop a model for this process and compare the results of the model to experimental data to extract kinetic parameters for the process.

Consider the schematic of Figure 3. A concentration gradient of excess Se (Ref. 9) exists across the CZTSe and MoSe$_2$ layers such that the concentrations of excess Se (in cm^{-3}) at the CZTSe upper surface, the CZTSe/MoSe$_2$ interface, and Mo/MoSe$_2$ interface are C_0, $C_{L1}(t)$, $C_{L2}(t)$, respectively. We assume that the concentration profile in between these points is linear. If the diffusional fluxes across the
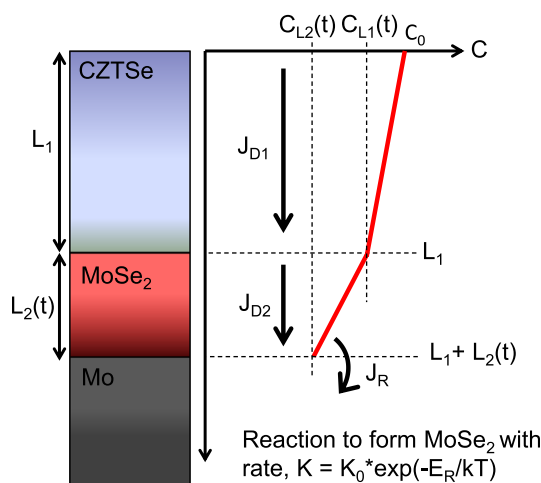
CZTSe layer, the MoSe$_2$ layer and the reaction flux at the Mo/MoSe$_2$ interface are J_{D1}, J_{D2}, and J_R, then

$$J_{D1} = -D_1 \frac{C_{L1}(t) - C_0}{L_1}, \tag{1a}$$

$$J_{D2} = -D_2 \frac{C_{L2}(t) - C_{L1}(t)}{L_2(t)}, \tag{1b}$$

$$J_R = K C_{L2}(t), \tag{1c}$$

$$J_{D1} = J_{D2} = J_R, \tag{1d}$$

where D_1, D_2, L_1, $L_2(t)$, and K are Se diffusivity across CZTSe, Se diffusivity across MoSe$_2$, thickness of the CZTSe layer, thickness of the MoSe$_2$ layer, and reaction rate (in cm/s), respectively. Because the partial pressure of Se during annealing is larger than the equilibrium vapor pressure of Se, a full coverage of Se adatoms on the CZTSe surface is assumed and the atomic density of metallic Se, $\sim 3.7 \times 10^{22}$ cm^{-3}, is used for C_0. Eliminating the fluxes, J_{D1}, J_{D2}, J_R, and $C_{L1}(t)$ from Eqs. (1a)–(1d) leads to

$$C_{L2}(t) = \frac{C_0}{\left(\frac{L_1}{D_1} + \frac{L_2(t)}{D_2}\right)K + 1}, \tag{2}$$

which reduces to C_0 when diffusion across the layer is much faster than the reaction rate, D_1/L_1 and $D_2/L_2 \gg K$ (i.e., reaction-limited) and to zero when $K \gg D_1/L_1$ and D_2/L_2 (i.e., diffusion-limited). The growth rate of MoSe$_2$ layer is given by

$$\frac{dL_2(t)}{dt} = \frac{J_R}{C'} = \frac{K C_{L2}(t)}{C'}, \tag{3}$$

where C' is the atomic concentration of Se in MoSe$_2$, $\sim 1.1 \times 10^{22}$ cm^{-3},[7] By combining Eqs. (2) and (3), we arrive at

$$\frac{dL_2(t)}{dt} = \frac{C_0}{C'} \frac{1}{\frac{L_1}{D_1} + \frac{L_2(t)}{D_2} + \frac{1}{K}}. \tag{4}$$

Solving Eq. (4) by the method of separation of variables[10] with the boundary condition of $L_2(0) = 0$, we obtain the following:

$$L_2(t) = \left(\frac{D_2}{K} + \frac{D_2 L_1}{D_1}\right)\left(\sqrt{1 + \frac{2\left(\frac{C_0}{C'}\right)K^2 D_1^2}{(D_1 + K L_1)^2 D_2}t} - 1\right). \tag{5}$$

In principle, Eq. (5) can be used to fit the experimental data (L_2 vs. annealing temperature or L_2 vs. annealing duration) with fitting parameters of D_1, D_2, and K. Because each of the fitting parameters consists of a prefactor and an activation energy, there are six fitting parameters.

For the case where Mo is selenized without a CZTSe layer, Eq. (5) simplifies to

$$L_2(t) = \frac{D_2}{K}\left(\sqrt{1 + 2\frac{C_0}{C'}\frac{K^2}{D_2}t} - 1\right), \tag{6}$$

FIG. 3. Schematic of excess Se concentration profile across CZTSe/MoSe$_2$/Mo during annealing in a steady-state.
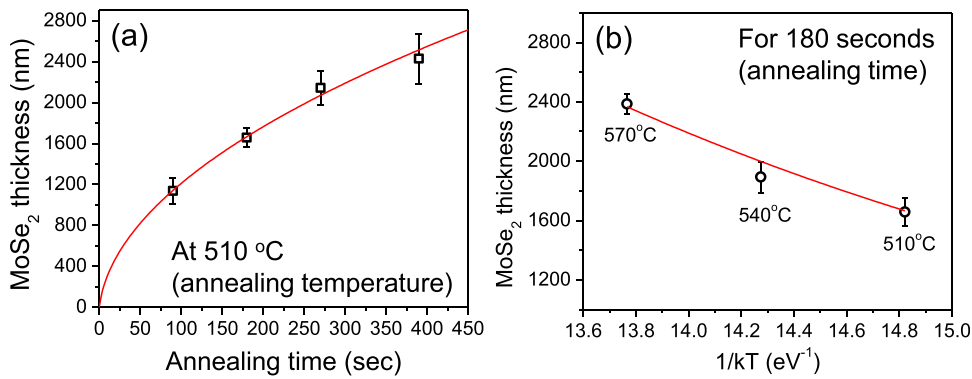
FIG. 4. Thickness of MoSe$_2$ formed on Mo-coated glass substrates annealed under Se atmosphere as function of (a) annealing time at a fixed annealing temperature, 510 °C and (b) annealing temperature for a fixed annealing duration, 180 s. The red curve is fit of the data by Eq. (6).

where symbols have the same meaning as in the case of CZTSe/MoSe$_2$/Mo. Under two extreme conditions, Eq. (6) reduces to (i) $L_2(t) \sim 2\frac{C_0}{C'}Kt$, when $2\frac{C_0}{C'}\frac{K^2}{D_2}t \ll 1$ (or K^{2}t $\ll$ D$_2$), i.e., reaction-limited and (ii) $L_2(t) = \sqrt{2\frac{C_0}{C'}D_2 t}$, when $2\frac{C_0}{C'}\frac{K^2}{D_2}t \gg 1$ (or K^{2}t $\gg$ D$_2$), i.e., diffusion-limited. Bare Mo-coated glass substrates without a CZTSe layer were annealed at various temperatures and for different annealing duration with the Se partial pressure kept larger than the equilibrium Se vapor pressure at each annealing temperature. Figures 4(a) and 4(b) present the measured MoSe$_2$ thickness as function of an annealing time (at a fixed annealing temperature, 510 °C) and an annealing temperature (at a fixed annealing duration, 180 s), respectively. By fitting Fig. 4(a) with Eq. (6) [red curve in Fig. 4(a)], K (at 510 °C) = K$_0$ exp($-$E$_R$/kT(= 783 K)) = 1.93($\pm$0.45) $\times 10^{-6}$ cm/s and D$_2$ (at 510 °C) = D$_{2,0}$ exp($-$E$_{D2}$/kT(= 783 K)) = 2.66($\pm$0.62) $\times 10^{-11}$ cm^2/s were obtained, where K$_0$ and D$_{2,0}$ are the prefactors, and E$_R$ and E$_{D2}$ are the activation energies for reaction and for Se diffusion across MoSe$_2$, respectively. With these results, Fig. 4(b) is fitted by Eq. (6) and the prefactor and the activation energy are now separately determined, see Table I. D$_{2,0}$ is smaller than the typical prefactors of bulk diffusivity by several orders of magnitudes, suggesting that grain boundary diffusion is a dominant transport mechanism of Se through the MoSe$_2$ layer. Then D$_{2,0}$ is related to δ_{MoSe2}*D$_{2,0(gb)}$/d$_{MoSe2}$, where δ_{MoSe2}, D$_{2,0(gb)}$, d$_{MoSe2}$ is the effective grain boundary thickness, the prefactor for grain boundary diffusivity, and the grain size of the MoSe$_2$, respectively.[11] The grain structure of the MoSe$_2$ appears to follow that of the underlying Mo layer consisting of columnar grains whose width ~50 nm. The prefactor that is grain size independent, δ_{MoSe2}*D$_{2,0(gb)}$ now becomes (2.8 $\pm$ 1.3) $\times 10^{-12}$ cm^3/s.

It becomes apparent from these results that within the range of temperature used in this study, K $\gg$ D$_2$/L$_2$ so that

the selenization of Mo is diffusion-limited. A similar study, where Mo films were selenized to form MoSe$_2$, has been reported in the literature.[12] In this study, the activation energy of MoSe$_2$ growth was determined 0.7 $\pm$ 0.1 eV by fitting a MoSe$_2$ thickness vs. temperature (1/T) with *a single exponent* over the entire annealing temperature range used (375–580 °C), implicitly assuming *a priori* that a limiting case—where one kinetic process is much slower than the others connected in series—was in play. Our finding that the process is diffusion-limited now supports their assumption and indeed their estimated activation energy of 0.7 $\pm$ 0.1 eV is very close to our estimation of E$_{D2}$.

Now, we revisit the CZTSe/MoSe$_2$/Mo case with four fitting parameters (D$_{2,0}$, E$_{D2}$, K$_0$, E$_R$) in Eq. (5) that are already determined. MoSe$_2$ thicknesses of CZTSe samples (with a constant CZTSe thickness of 1.5 μm) annealed at different temperatures are plotted in Fig. 5. D$_1$ can now be determined from fitting the data with Eq. (5) with the pre-determined D$_2$ and K from the selenization of Mo layers discussed earlier; D$_{1,0}$ = (5.0 $\pm$ 1.0) $\times 10^{-6}$ cm^2/s and E$_{D1}$ = 0.69 $\pm$ 0.12 eV. Similar to the case of selenization of the Mo, the value of D$_{1,0}$ suggests that grain boundary diffusion is dominant over bulk diffusion. D$_1$ is given by $D_1 = \frac{\delta_{CZTSe}D_{1,0(gb)}}{d_{CZTSe}}\exp\left(-\frac{E_{D2}}{kT}\right)$, where δ_{CZTSe}, D$_{1,0(gb)}$, d$_{CZTSe}$ are the effective grain boundary thickness, the prefactor for grain boundary diffusivity, and the size of CZTSe grains, respectively. Grain growth in the CZTSe layer takes place during annealing and therefore d$_{CZTSe}$ here is not constant but time-dependent and temperature-dependent. For more
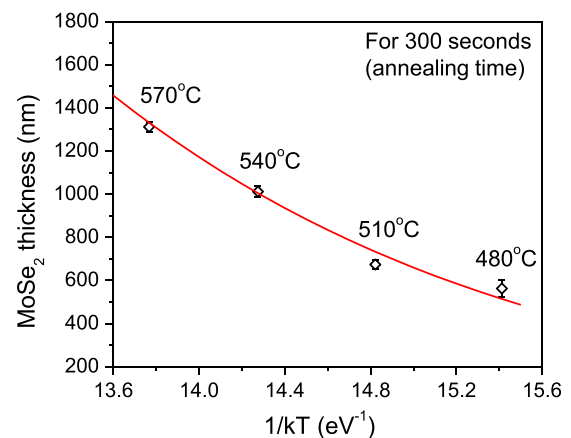
TABLE I. Kinetic parameters of Se diffusion through CZTSe and Mo, and of MoSe$_2$ formation.

	Prefactor	Activation energy [eV]
Se diffusion in CZTSe (D$_1$)	D$_{1,0}$ = (5.0 $\pm$ 2.0) $\times 10^{-6}$ cm^2/s	E$_{D1}$ = 0.69 $\pm$ 0.24
Se diffusion in MoSe$_2$ (D$_2$)	D$_{2,0}$ = (5.5 $\pm$ 2.6) $\times 10^{-7}$ cm^2/s	E$_{D2}$ = 0.68 $\pm$ 0.34
Reaction to form MoSe$_2$ (K)	K$_0$ = (2.5 $\pm$ 0.9) $\times 10^{-2}$ cm/s	E$_R$ = 0.33 $\pm$ 0.20

FIG. 5. Thickness of MoSe$_2$ formed between CZTSe and Mo as function of annealing temperature for a fixed annealing duration, 300 s. The red curve is fit of the data by Eq. (5).

accurate fitting of the experimental results, the time- and temperature-dependence of $D_{1,0}$ should be explicitly considered in solving Eq. (4), which we leave for the future work because we currently lack the knowledge on the evolution of CZTSe grain structure as function of time and temperature. Nevertheless, considering all kinetic parameters, we now find that $K \gg D_1/L_1 > D_2/L_2$ for the temperature range of our practical interest, revealing that the $MoSe_2$ formation in $CZTSe/(MoSe_2)/Mo$ is mainly limited by the diffusion through the CZTSe layer. The kinetic parameters that we extract from this study are now summarized in Table I.

In summary, we have studied the kinetics of $MoSe_2$ formation between Mo and CZTSe films during annealing under Se ambient. The formation of $MoSe_2$ in this system is modeled with three step processes—diffusion of Se through CZTSe, diffusion through $MoSe_2$ which is growing with continued annealing, and reaction between Se and Mo. An analytical formula that relates $MoSe_2$ interfacial layer thickness with kinetic parameters (D_1, D_2, and K) is derived. First, selenization of Mo layers without the CZTSe is examined, from which D_2 and K are determined. Now with D_2 and K are known, D_1 is determined by fitting $MoSe_2$ thickness vs. annealing temperature of $CZTSe/MoSe_2/Mo$ samples with the derived formula. Comparison of the kinetic parameters ($K \gg D_1/L_1 > D_2/L_2$) reveals that the $MoSe_2$ formation occurring during high temperature process of a CZTSe thin film solar cell is limited by the diffusion of Se through the CZTSe layer.

[1]B. Shin, Y. Zhu, N. A. Bojarczuk, S. J. Chey, and S. Guha, Appl. Phys. Lett. **101**, 053903 (2012).

[2]B. Shin, O. Gunawan, Y. Zhu, N. A. Bojarczuk, S. J. Chey, and S. Guha, Prog. Photovoltaics **21**, 72 (2013).

[3]S. Bag, O. Gunawan, T. Gokmen, Y. Zhu, T. K. Todorov, and D. B. Mitzi, Environ. Sci. Technol. **5**, 7060 (2012); D. A. R. Barkhouse, O. Gunawan, T. Gokmen, T. K. Todorov, and D. B. Mitzi, Prog. Photovoltaics **20**, 6 (2011); I. Repins, C. Beall, N. Vora, C. DeHart, D. Kuciauskas, P. Dippo, B. To, J. Mann, W.-C. Hsu, A. Goodrich, and R. Noufi, Sol. Energy Mater. Sol. Cells **101**, 154 (2012).

[4]S. Nishiwaki, N. Kohara, T. Negami, and T. Wada, Jpn. J. Appl. Phys., Part 2 **37**, L71 (1998).

[5]X. Zhu, Z. Zhou, Y. Wang, L. Zhang, A. Li, and F. Huang, Sol. Energy Mater. Sol. Cells **101**, 57 (2012).

[6]The Mo coating on a glass substrate was prepared by four separate scans of sputtering of Mo, hence, different contrasts between four layers are seen in the Mo layer from SEM images. In Fig. 1(a), we can see that an upper part of the top Mo layer was converted to $MoSe_2$.

[7]P. B. James and M. T. Lavik, Acta Cryst. **16**, 1183 (1963).

[8]It is obvious that the diffusing species in the CZTSe is Se, not Mo, because otherwise the $MoSe_2$ layer would form on top of the CZTSe. So it can be inferred that Se is much faster than Mo in the CZTSe. It is conceivable that the same is true for the $MoSe_2$ layer and we presume that the diffusing species in the $MoSe_2$ is also Se, not Mo. The results are insensitive to the identity of diffusing species in the $MoSe_2$ layer; however, the interpretation of the parameters such as diffusivity is dependent on the assumption.

[9]Our definition of "excess Se" is selenium that does not participate in forming the CZTSe or $MoSe_2$ compound and that is present only when there is an external source of Se (i.e., Se vapor introduced during the annealing).

[10]P. D. Ritger and N. J. Rose, *Differential Equations with Application* (McGraw-Hill, 1968).

[11]Y. Mishin and C. Herzig, Mater. Sci. Eng., A **A260**, 55 (1999).

[12]L. Kaupmess, M. Altosaar, O. Volobujeva, T. Raadik, M. Grossberg, M. Danilson, E. Mellikov, and P. Barvinschi, Adv. Mater. Sci. Eng. **2012**, 345762.